INTERFEROMETRIC SAS: A COMPARISON OF SIMULATED AND EXPERIMENTAL RESULTS

A. J. Hunter, P. T. Gough, and M. P. Hayes

Acoustics Research Group, Department of Electrical and Computer Engineering,
University of Canterbury, Private Bag 4800, Christchurch, New Zealand
{a.hunter, p.gough, m.hayes}@elec.canterbury.ac.nz

1. INTRODUCTION

Ground-truth is difficult to obtain in the ocean environment. Optical visibility is typically no more than a few metres and sufficiently accurate surveys are unfeasible. Known targets can be deployed. However, the structure and properties of the seafloor and water column are generally unknown. It is difficult to assess the performance of synthetic aperture sonar (SAS) algorithms without accurate ground-truth.

Simulated data provides a means of assessing SAS algorithm performance. A known model of a scene is used to generate the echo data. Thus, the model can be used to provide the ground-truth. However, the validity of this approach is dependent on the accuracy of the simulator.

Experimental data was obtained in recent sea-trials using our interferometric SAS (InSAS) [1]. Accurate ground-truth for the imaged region was unavailable. However, a 3-dimensional bathymetric reconstruction provides an estimate of the topography [2]. This can be used as a scene model for the simulator [3–5] and a simulated data set can be obtained for comparison. The comparison between the simulated and experimental data is presented in this paper.

Comparison between the simulated and experimental imagery provides a means of evaluating the performance of the SAS and bathymetry algorithms as well as the simulator. If the imagery is identical then it indicates that the forward and inverse models are consistent with each other; differences between the images indicate errors in either the forward or inverse models. In theory, the errors due to the forward model can be reduced and inconsistencies between the two data sets can be attributed to the inverse model. Ultimately, the simulator could be used as a feedback path within an iterative algorithm, closing the loop in the simulation/reconstruction process.

2. LYTTELTON HARBOUR SEA-TRIALS

Two sea-trials were conducted in February and March of 2006 using a single-pass InSAS (KiwiSAS-IV) [1] in Lyttelton Harbour, Canterbury, New Zealand. Parson's Rock is a feature of interest in the imagery from the trials. It is a volcanic rock mass that protrudes up to 6 m from the surrounding silt/sand seafloor at an average depth of 10 m. While ground-truth for the region is unavailable, the protruding rock appears to be some 50 m by 50 m in extent. The rock was imaged at a range of approximately 25 m with the towfish traveling mid-water, imaging the swath in a side-scan geometry as shown in Fig. 1.

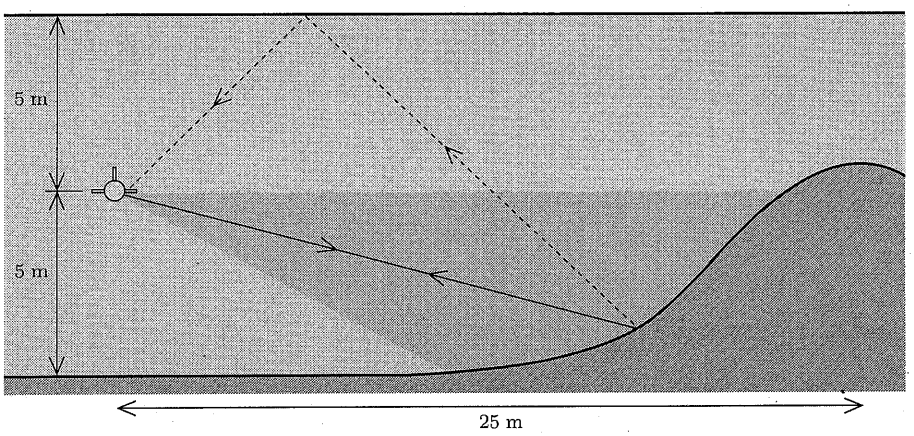

Figure 1: Parson's Rock is a volcanic rock mass that protrudes up to 6 m from the surrounding silt/sand seafloor at an average depth of 10 m. The rock was imaged in a side-scan geometry at a range of approximately 25 m. The close proximity of the sea surface results in significant multipath scattering. The projector is tilted down by 12 deg in an effort to reduce the sea surface multipath.

The KiwiSAS is a free-towed sonar. A single projector (transmitter) and a 3×3 hydrophone (receiver) array are located on the starboard side of the towfish. The projector is tilted down by 12 deg in an effort to reduce multipath reflections from the sea surface. The sonar transmits two linear FM chirp signals at a ping rate of 15 Hz. The signals have a bandwidth of 20 kHz each with centre frequencies of 30 kHz and 100 kHz. They are transmitted and received simultaneously using the same projector and hydrophones. This yields multi-frequency imagery of the swath that is geometrically identical [6]. The theoretical resolution of the imagery after matched filtering and synthetic aperture processing is approximately 5 cm in range by 15 cm in along-track.

The SAS imagery from a run during the February sea-trial is shown in Fig. 2 for the two frequency bands. The imagery was reconstructed using the wavenumber algorithm [7] assuming a linear trajectory and a constant speed of 1 m/s. Navigation data was unavailable for the trials and any deviations from the linear trajectory are left uncorrected. Localised along-track blurring is evident in the imagery; this is thought to be due to variations in the towfish speed. The along-track *banding*, which is evident in the 100 kHz imagery, is an indication of roll; this has an affect on the interferometric phase estimation. It is likely that other deviations are also present. These uncompensated motions reduce the image resolution, introduce geometrical distortions, and cause reconstruction artefacts. It is important to note that the 30 kHz imagery appears noisier than the 100 kHz imagery. This could be due to multipath scattering from the sea surface and/or due to sub-surface penetration and volume scattering.

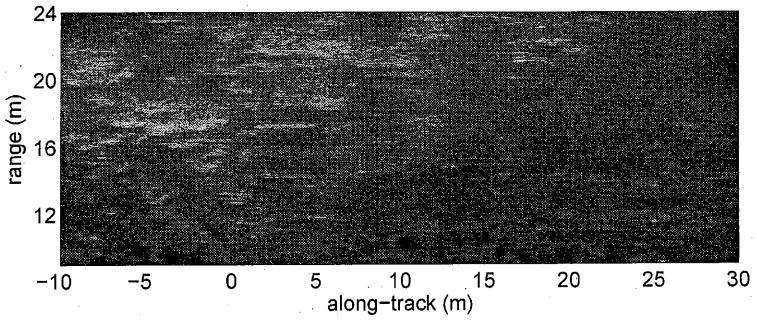

(a) 30 kHz SAS imagery

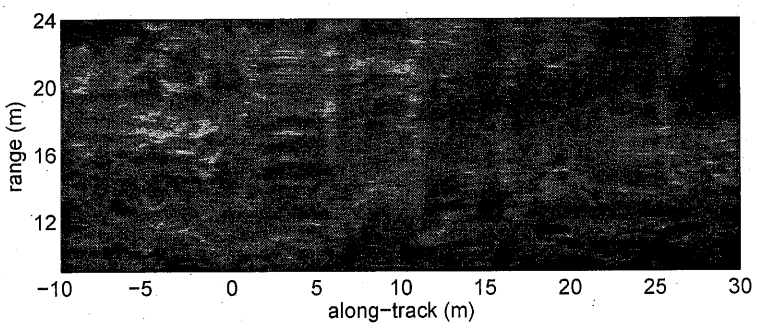

(b) 100 kHz SAS imagery

Figure 2: Multi-frequency InSAS imagery of Parson's Rock was obtained by the KiwiSAS-IV. The imagery shows the rock on the left hand side receding into the sea floor on the right.

3. BATHYMETRIC RESULTS

The hydrophone array provides a vertically separated set of 3 hydrophones for interferometry. Time delays between the hydrophones can be used to estimate the angle of arrival and infer the seafloor topography. The reconstructed imagery from the three hydrophones and two frequency bands are combined in a maximum likelihood (ML) estimate. Multiple frequency sub-bands and azimuth looks are used to sacrifice resolution for reduced variance in the height estimate [2].

A bathymetric reconstruction of the experimental data was performed using 9 frequency sub-bands and 5 azimuth looks. Erroneous spikes in the heightmap due to phase wrapping and low coherence were removed by thresholding and the heightmap was repaired using Delaunay triangulation [8]. The resultant heightmap is shown in Fig. 3(a); the resolution is approximately 50 cm by 75 cm (across-track $\times$ along-track). Parson's Rock is evident on the left hand side, reaching a height of approximately 6 m above the seafloor.

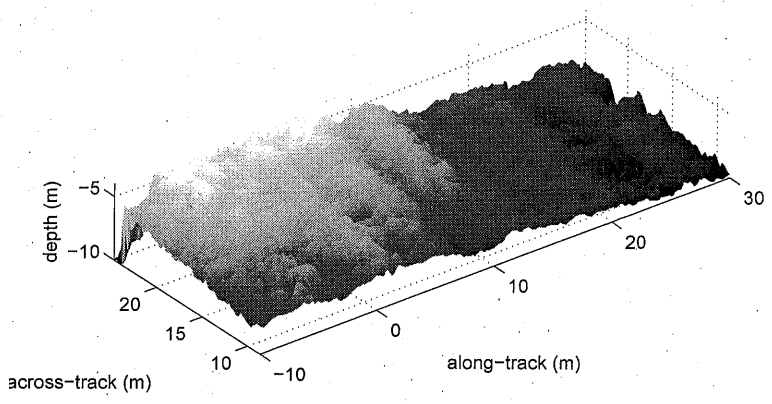

(a) Full resolution heightmap

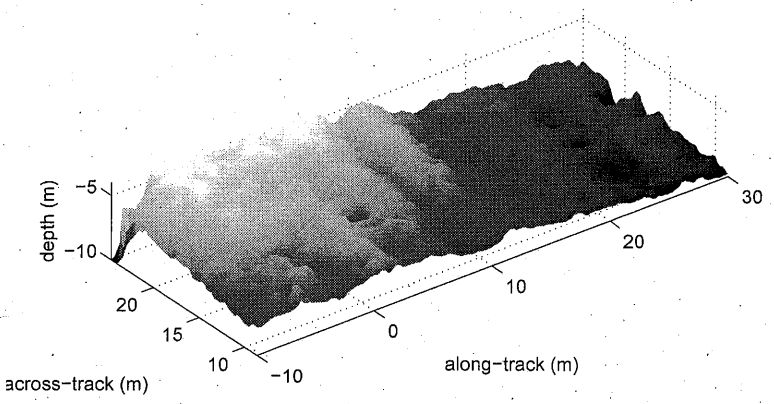

(b) Median filtered heightmap

Figure 3: A heightmap of Parson's Rock was obtained using a maximum likelihood estimate of the time delay between hydrophones in the interferometric array. The heightmap is smoothed using a $0.5\ \mathrm{m} \times 0.5\ \mathrm{m}$ median filter to remove speckle artefacts.

The heightmap exhibits a series of ridges; these correlate with the banding in the $100\ \mathrm{kHz}$ imagery. It is probable that these ridges are not a feature of the seafloor but an artefact due to interferometric phase errors from the uncompensated roll. The heightmap also exhibits high-frequency variations that are commensurate with the speckle in the imagery (after filtering). It is unlikely that these variations are an actual feature of the seafloor.

4. SIMULATED RESULTS

There are a number of simulators in the literature for SAS [9, 10] and SAR [11]; these typically use a point and/or facet decomposition of the surfaces in the scene. The simulator employed here decomposes the scene into rough, instead of smooth, facets. This is more efficient since the small-scale roughness does not need to be modelled explicitly and the scene can be decomposed into fewer facets. The scattering from each facet is modelled using an extension of the Kirchhoff approximation [3]. Each facet is characterised by its shape, position, and orientation, the properties of the medium on each face, and the statistics of the small-scale surface roughness. The facet response is realised from an analytic expression for the scattered field statistics and the imagery is obtained by summation of the visible facet responses, where occlusions and multiple scattering are resolved by ray-tracing [5]. The simulator is implemented for parallel operation on a computing cluster [4].

The bathymetric heightmap generated from the sea-trial data is used as an input mesh for the simulator. The heightmap is tessellated into a collection of triangles with along/across-track dimensions of $15\ \mathrm{cm}$ by $15\ \mathrm{cm}$, yielding a mesh of approximately 50000 facets. The properties of rock are assumed for the seafloor, with a sound speed of $6000\ \mathrm{m/s}$ and a density of $3000\ \mathrm{kg/m^3}$ estimated from empirical data. The surface roughness is assumed to be Gaussian distributed and Gaussian correlated with a height variance on order of a wavelength at $30\ \mathrm{kHz}$ and a correlation length small compared to the extents of the facets. The raw echo data is generated by the simulator using a linear towpath at a speed of $1\ \mathrm{m/s}$ and a depth of $5\ \mathrm{m}$.

The simulated SAS imagery (after matched filtering and synthetic aperture processing) is shown in Fig. 4 for the two frequency bands. A comparison with the experimental imagery in Fig. 2 shows significant differences. Most notably, the simulated imagery has a higher resolution and the seafloor appears to have higher spatial frequency content. The simulated data does not exhibit the same artefacts due to uncompensated towpath deviations and the experimental data appears noisier. However, the beampattern nulls in the simulated and experimental imagery appear in the same locations; this indicates that the underlying structure of bathymetric heightmap is correct.

The heightmap is filtered to remove the speckle artefacts using a $0.5\ \mathrm{m} \times 0.5\ \mathrm{m}$ median filter. The simulated imagery using the filtered heightmap is shown in Fig. 5. This imagery resembles the experimental data more closely. However, the simulated and experimental imagery are far from identical.

5. DISCUSSION

It is envisaged that a simulator could be used in a closed-loop process to assess and improve the quality of SAS image reconstruction. The bathymetric heightmap can be used as an input to the simulator and the simulated imagery can be compared with the experimental imagery to give a quality metric; the metric is maximised when the imagery is identical, indicating an accurate reconstruction. That is, assuming the simulator is perfect. The reconstruction and simulation parameters can be altered to maximise the quality metric in an iterative process until the simulated and experimental imagery are identical. A possible metric for the image comparison is the mean square error. The proposed closed-loop reconstructor is illustrated in Fig. 6.

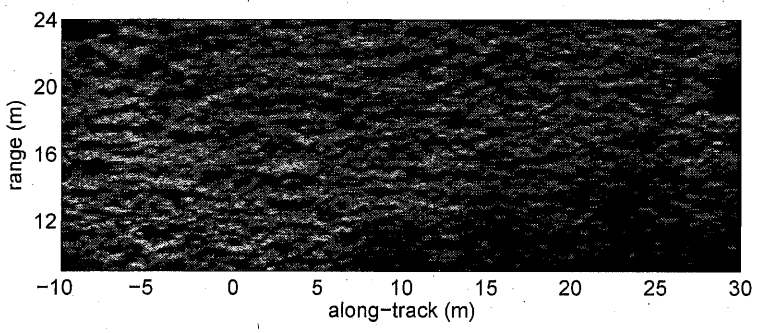

(a) 30 kHz simulation

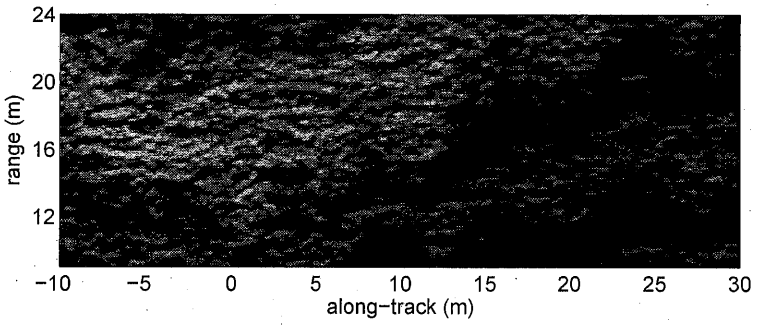

(b) 100 kHz simulation

Figure 4: SAS imagery of Parson's Rock was simulated using the bathymetric heightmap obtained from the experimental data. The simulated imagery exhibits higher resolution and higher spatial frequency content than the experimental imagery.

6. CONCLUSIONS AND FUTURE WORK

Significant disparity between the simulated and experimental imagery is observed. This is indicative of errors in the reconstruction and/or simulation process. The forward and inverse models employ simplifying approximations that contributes to these errors. The towfish navigation data was unavailable and, consequently, the unknown deviations from an assumed linear towpath were left uncompensated; this is thought to be the biggest source of error. In addition, certain aspects were neglected in the simulations including multipath scattering, sub-surface penetration, and volume scattering.

The bathymetric heightmap exhibits high frequency variations that are thought to be due to speckle. Filtering the heightmap removed the speckle artefacts and provided a closer match between the simulated and experimental imagery. However, significant disparity between the

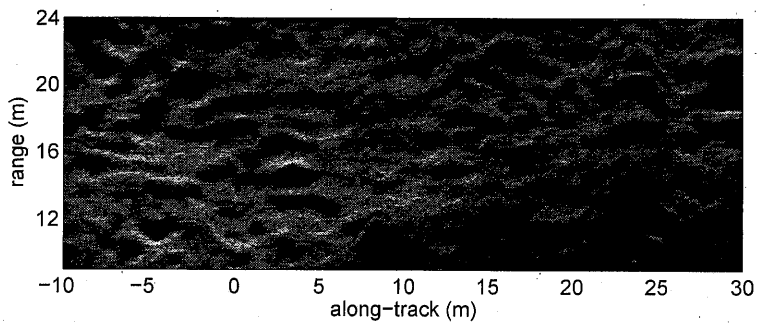

(a) 30 kHz simulation

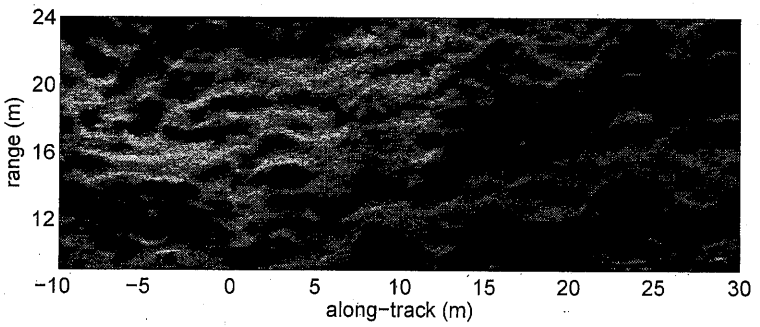

(b) 100 kHz simulation

Figure 5: The median filtered heightmap does not exhibit the speckle artefacts and the simulated imagery resembles the experimental imagery more closely.

simulated and experimental imagery remains. Modifying the reconstruction parameters (in this case, by filtering the bathymetric heightmap) based on a comparison between the simulated and experimental imagery has provided a more accurate result. This indicates that a comparison of simulated and experimental imagery could be used to determine a quality metric. A closed-loop reconstruction algorithm is proposed based on these preliminary results.

To further assess the validity of the approach, the sources of error due to towpath deviations must be removed. This can be achieved using an INS in a future sea trial or using autofocus techniques. Ideally, errors due to approximations in the forward model will be further reduced. The proposed closed-loop reconstruction scheme is unfeasible at present due to the computational requirements of the simulation stage. However, the scheme should become feasible in the future with the continued advance in computing power.

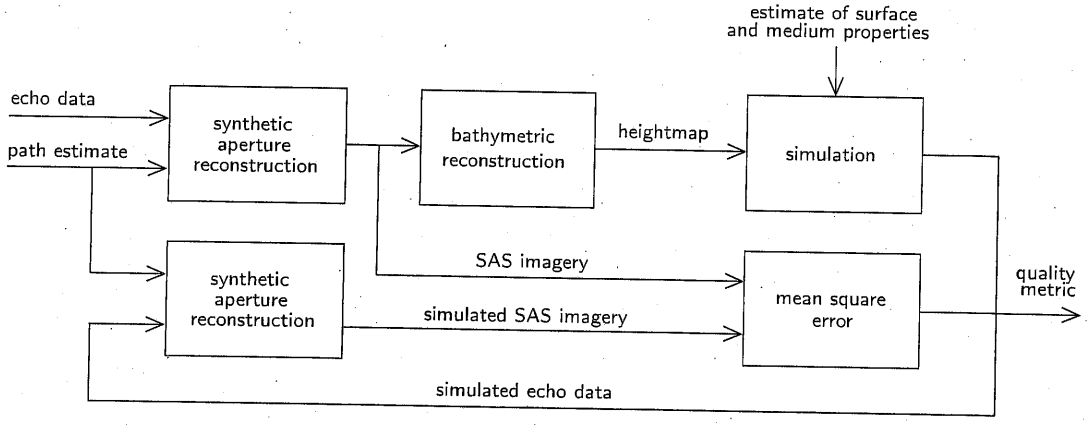

Figure 6: The proposed iterative SAS reconstruction algorithm employs a simulator in a feedback path. The difference between the simulated and experimental imagery provides a quality metric for the process.

REFERENCES

[1] M. P. Hayes, P. J. Barclay, and P. T. Gough. Test results from a multiple-baseline interferometric synthetic aperture sonar. In *ECUA 2006*, Portugal, June 2006. ECUA.

[2] P. J. Barclay, M. P. Hayes, and P. T. Gough. ML estimation of seafloor topography using multi-frequency synthetic aperture sonar. In *Oceans 2005*, Brest, France, July 2005. IEEE.

[3] A. J. Hunter, M. P. Hayes, and P. T. Gough. Simulation of multiple-receiver, broadband interferometric SAS imagery. In *Oceans 2003*, San Diego, USA, September 2003. IEEE/MTS.

[4] A. J. Hunter and M. P. Hayes. A distributed acoustic renderer for SAS image simulation. In *IVCNZ 2004*, pages 333–338, Akaroa, New Zealand, November 2004.

[5] A. J. Hunter and M. P. Hayes. Towards more accurate shadow modelling for simulated SAS imagery. In *Oceans 2005*, Brest, France, June 2005. IEEE.

[6] M. A. Noonchester, P. T. Gough, A. J. Hunter, and M. P. Hayes. Imagery from a multi-frequency SAS: a comparison of simulated and experimental results. In *IOA 2006*, Lerici, Italy, September 2006. IOA.

[7] P. T. Gough and M. P. Hayes. Fast Fourier techniques for synthetic aperture sonars. In *Oceans 2005*, Brest, France, June 2005.

[8] F. P. Preparata and M. I. Shamos. *Computational Geometry: An Introduction*. Springer-Verlag, 1985.

[9] J. Groen, B. A. J. Quesson, J. C. Sabel, R. E. Hansen, H. J. Callow, and T. O. Sæbø. Simulation of high resolution mine hunting sonar measurements. In *Proc. Underwater Acoustic Measurements*, Crete, Greece, July 2005.

[10] G. S. Sammelmann. High frequency images of proud and buried 3-D targets. In *OCEANS 2003*, pages 266–272, San Diego, California, September 2003. IEEE.

[11] G. Franceschetti, A. Iodice, M. Migliaccio, and D. Riccio. A novel across-track SAR interferometry simulator. *IEEE Trans. Geoscience and Remote Sensing*, 36(3):950–962, May 1998.